Journal of Cellular Biochemistry 104:213–223 (2008)

Expression of Iron-Related Proteins During Infection by Bovine Herpes Virus Type-1

Carmen Maffettone,[1] Luisa De Martino,[2] Carlo Irace,[1] Rita Santamaria,[1]* Ugo Pagnini,[2] Giuseppe Iovane,[2] and Alfredo Colonna[1]

[1]Dipartimento di Farmacologia Sperimentale, Università di Napoli Federico II, via D. Montesano 49, I-80131 Napoli, Italy
[2]Dipartimento di Patologia e Sanità Animale, Università di Napoli Federico II, via F. Delpino 1, I-80137 Napoli, Italy

Abstract Bovine herpesvirus 1 (BHV-1), a dsDNA animal virus, is an economically important pathogen of cattle and the aetiological agent of many types of disease. The efficient replication of a DNA virus is strictly dependent on iron since this metal plays a crucial role in the catalytic center of viral ribonucleotide reductase. Consequently, iron metabolism is an important area for virus/host interaction and a large body of evidence suggests that viral infection is potentially influenced by the iron status of the host. The aim of the present study was to address the effects of BHV-1 on iron metabolism in Madin-Darby bovine kidney (MDBK) cells at different times of post-infection. For this purpose, cell viability, iron regulatory proteins (IRPs) activity and levels, transferrin receptor 1 (TfR-1), ferritin expression and LIP were evaluated. Our data demonstrate that a productive BHV-1 infection in MDBK cells determines an overall decrease of IRPs RNA-binding activity without affecting their expression. As consequence of this modulation, an increased ferritin mRNA translation and a decreased TfR-1 mRNA translation were also observed. Moreover, the LIP level was decreased following viral infection. These results are consistent with the hypothesis that by reducing the iron up-take and by enhancing the sequestration of free iron, animal cells will limit the iron availability for virus proliferation. Therefore, the results presented herein support the view that iron metabolism could be critical for the interaction between DNA viruses, such as BHV-1, and mammalian cells. Delineation of the interplay among pathogen and host may provide new antimicrobial agents. J. Cell. Biochem. 104: 213–223, 2008.

Key words: bovine herpes virus type-1; iron metabolism; iron regulatory proteins; ferritin; transferrin receptor; labile iron pool

Iron is an essential element for all living cells due to its critical role as a component of prosthetic groups in a variety of enzymes and electron transfer proteins [Aisen et al., 1999], yet at the same time iron is potentially cytotoxic. Cytotoxicity is due to the ability by which free iron, as Fe^{2+} ions, participates in redox reactions leading to the production of harmful oxygen radicals [Nelson and McCord, 1998]. Consequently, to suppress the potential deleterious effects of iron, cells have evolved homeostatic mechanisms that regulate transport, storage and mobilisation of this essential element.

In mammals, most iron is found within cells, complexed to haemoglobin in erythrocytes or to the ubiquitous intracellular iron storage protein ferritin, a multimer constituted of heavy (H) and light (L) subunits [Harrison and Arosio, 1996]. Extracellular iron is bound to transferrin (Tf), which shuttles iron through the blood to target tissues. Mono- and diferric-transferrin bind to the Tf-receptor (TfR), that transports iron into the cell via clathrin-coated pits [Fishman et al., 1987]. At the cellular level, the maintenance of iron homeostasis is largely accomplished by the

Abbreviations used: BHV-1, bovine herpes virus type-1; MDBK, Madin-Darby bovine kidney; MOI, multiplicity of infection; MTT, 3-(4,5-dimethyl-2-thiazolyl)-2,5-diphenyl-2*H*-tetrazolium bromide; IRPs, iron regulatory proteins; TfR-1, transferrin receptor-1; 2-ME, 2-mercaptoethanol; LIP, labile iron pool; CA, calcein; BIP, 2,2′-bipyridil.

*Correspondence to: Rita Santamaria, Dipartimento di Farmacologia Sperimentale, Università di Napoli Federico II, via D. Montesano 49, I-80131 Napoli, Italy.
E-mail: rsantama@unina.it

Received 26 April 2007; Accepted 24 September 2007
DOI 10.1002/jcb.21618

TfR-1, which regulates iron uptake, and by ferritin, which is crucial to keep this metal in a non-toxic form. The levels of these and other proteins involved in iron metabolism are mainly regulated post-transcriptionally by interaction between the iron regulatory proteins (IRP-1 and IRP-2) and stem-loop structures, termed iron responsive elements (IREs), located in the 5′ untranslated region (UTR) of ferritin mRNAs and in the 3′ UTR of transferrin receptor mRNA [Pantopoulos, 2004; Wallander et al., 2006]. IRP-1, the cytosolic counterpart of mitochondrial aconitase [Kennedy et al., 1992], is a bifunctional protein that, through [4Fe-4S] cluster assembly/disassembly, switches from the aconitase to the IRP-1 form mainly in response to the intracellular iron level. IRP-2 is homologous to IRP-1 but lacks the [4Fe-4S] cluster and its activity increases in iron-depleted cells by protein stabilisation [Guo et al., 1994].

The so-called labile iron pool (LIP), which is often referred to as the low-molecular-weight transit iron pool or chelatable iron, regulates IRP-1 by affecting its RNA-binding capacity and IRP-2 by inducing its degradation [Guo et al., 1995; Henderson and Kühn, 1995]. In particular, when intracellular iron content decreases, IRPs interact with multiple IREs within the 3′-UTR of TfR-1 mRNA, thereby strongly increasing mRNA half-life and TfR-1 protein expression at the cell surface [Müllner et al., 1989]. Simultaneously, the binding of IRPs to IRE *cis*-element in the 5′-UTR of ferritin mRNA interferes with the assembly of functional 80S translation initiation complexes thereby preventing protein synthesis [Aziz and Munro, 1987; Hentze et al., 1987]. On the other hand, high iron levels reduce IRPs affinity to IREs (i.e. IRP-1 is no longer able to bind IRE and IRP-2 is degraded), resulting in rapid transferrin receptor mRNA degradation and in efficient translation of ferritin [Eisenstein, 2000]. The IRPs RNA-binding activity is also regulated by other factors, such as oxidative stress [Pantopoulos et al., 1997], nitric oxide signalling [Drapier et al., 1993], protein phosphorylation [Brown et al., 1998], hypoxia [Meyron-Holtz et al., 2004; Irace et al., 2005] as well as oxalomalic acid, a known inhibitor of aconitase/IRP1 [Festa et al., 2000b; Santamaria et al., 2004, 2006].

BHV-1, a member of the *Alphaherpesvirinae* subfamily, is an important pathogen of cattle and the aetiological agent of many disease types such as severe respiratory infection, conjunctivitis, infectious pustular vulvovaginitis, balanoposthitis, abortion and systemic infection in neonate calves. BHV-1 shows high prevalence in cattle herds all over the world, and furthermore, like all members of the family Herpesviridae, establishes a latent infection in sensory ganglionic neurons of an infected host [Jones, 2003]. Moreover, BHV-1 may predispose infected animals, possibly through immunosuppression, to secondary bacterial infections.

Herpesviruses are enveloped large double-stranded DNA viruses with the genome ranging in size from 80 to 250 kb, and the subfamily *Alphaherpesvirinae* contains between 70 and 80 protein-coding genes [Roizman and Pellet, 2001]. Specifically, the genome of BHV-1 (Cooper strain), which has been completely sequenced, is 135,301 bp in length and contains an estimated 73 genes (GenBank accession number AJ004801). The genome consists of two unique sequences, long or UL (103 kb L segment) and short or US (32 kb S segment), comprising a 10-kb unique region flanked by 11 kb internal and terminal inverted repeats. This arrangement corresponds to the D-type herpesviral genome [McGeoch and Davison, 1999]. Despite increasing knowledge of genome structure and individual viral proteins, studies on virus replication and pathogenesis are not yet completely clear.

It is known that viral infections are influenced by the iron status of the host [Weiss et al., 1999; Kakizaki et al., 2000; Clark and Semba, 2001] and the replication of DNA virus requires dNTPs supplied by a viral ribonucleotide reductase (RR) [Stubbe, 1990]. Consequently, DNA viruses are directly dependent on iron for their proliferation since this metal plays a crucial role in the catalytic center of RR, which consists in an heterodimeric protein containing a di-iron prosthetic group [Cooper et al., 1996; Lamarche et al., 1996; Chabes et al., 2000]. Viral RR is an early gene product encoded by most if not all DNA viruses (e.g. pox, vaccinia and herpes simplex viruses) [Howell et al., 1993]. Moreover, in in vitro experiments iron status has been reported to influence viral replication and recently it has become evident that manipulation of host iron status leads to a modulation of the proliferation and virulence of many microorganisms [Cinatl et al., 1994; Richardson, 1997; Darnell and Richardson, 1999; Van Asbeck et al., 2001]. Thus, changes in iron homeostasis have been implicated in the pathogenesis of several DNA and RNA viruses.

However, to the authors' knowledge, iron metabolism in the bovine herpesvirus type-1 (BHV-1) infection has not yet been investigated. The present study was undertaken to investigate the cellular regulation of iron metabolism during animal DNA virus infection. In particular, we focused on an in vitro model system of BHV-1 infection, and on the possible impact of the IRPs activity and TfR-1 and ferritin expression on iron homeostasis and on the disease progression.

MATERIALS AND METHODS

Virus and Culture Conditions

The reference BHV-1 Cooper strain was used in this study. It was routinely grown on Madin-Darby bovine kidney cells (MDBK, American Type Culture Collection CCL22) cultured in Dulbecco's modified Eagle's medium (DMEM) (Eurobio, France) supplemented with 2 mM L-glutamine (Bio-Whittaker), 1% non-essential aminoacids, 5% pre-screened and heat-inactivated foetal calf serum (FCS) (Eurobio), 100 U of penicillin and 100 μg of streptomycin per ml (both antibiotics from Bio-Whittaker), at 37°C in a humidified 5% CO_2 atmosphere. This cell line was maintained free of mycoplasma and of bovine viral diarrhoea virus.

MDBK cells were also used for determination of virus titres and virus stocks with titres of 2×10^7 $TCID_{50}$ ml^{-1} were stored in liquid nitrogen until use.

Cell Viability and Microscopy

Cell viability after BHV-1 infection was monitored by evaluation of mitochondrial suffering through the MTT assay. MDBK cells were seeded in 25 cm^2 culture flasks at a density of 3×10^6 cells per flask, infected or not with BHV-1 at different multiplicity of infection (MOI), precisely 0.01, 0.1, 1 and 10 MOI, in a small volume of culture medium without FCS for 1 h at 37°C with moderate shaking. Then the inocula were removed and the infected monolayers were incubated up to 48 h in DMEM supplemented with 2 mM L-glutamine, 1% non-essential aminoacids, 5% FCS, 100 U of penicillin and 100 μg of streptomycin per ml, at 37°C in a humidified 5% CO_2 atmosphere. Briefly, MTT solution [3-(4,5-dimethyl-2-thiazolyl)-2,5-diphenyl-2*H*-tetrazolium bromide] (Sigma–Aldrich, St. Louis, MO) was added to BHV-1 infected cells and after 4 h of incubation the medium was removed and replaced with DMSO to solubilize the MTT formazan crystals. The absorbance was monitored at 570 nm using a Perkin-Elmer LS 55 Luminescence Spectrometer (Perkin-Elmer Ltd., Beaconsfield, UK). Data are expressed as a percentage of the control, and results are the mean ± SD of three experiments performed in duplicate.

In microphotography experiments, cells were grown on 100 mm standard culture dishes (Tissue Culture Dish, Falcon) by plating 3×10^6 cells in 10 ml of culture medium (see above). After reaching confluence, cells were infected with BHV-1 for different times at a MOI of 1 and finally placed on a contrast-phase light microscope (Labovert microscope, Leizt). Microphotographs at a 100× magnification were taken with a standard VCR camera (Nikon).

Virus Infection

Monolayers of MDBK cells were either mock infected with medium alone or infected with BHV-1 Cooper at a multiplicity of infection of 1 $TICD_{50}$/cell in culture medium lacking FCS. Virus inoculum was allowed to proceed for 1 h at room temperature. After removal of the inoculum, the monolayers were overlaid with prewarmed medium (DMEM containing 2 mM L-glutamine and 2% FCS) and incubated at 37°C in humidified 5% CO_2 atmosphere. At the end of various incubation times, the monolayers were collected by scraping and low-speed centrifugation and used for the different experimental procedures.

Preparation of Cellular Extracts

After established times of BHV-1 infection, MDBK cells were washed and scraped off with PBS containing 1 mM EDTA. To obtain cytosolic extracts for electrophoretic mobility-shift assay (EMSA), cells were lysed at 4°C with buffer containing 10 mM HEPES, pH 7.5, 3 mM $MgCl_2$, 40 mM KCl, 5% (v/v) glycerol, 1 mM dithiothreitol (DTT), 0.2% (v/v) Nonidet P-40 (NP-40) and serine and cysteine proteases inhibitors cocktail tablets (complete mini EDTA-free, Roche, Mannheim, Germany). Cell debris and nuclei were pelleted by centrifugation at 15,000*g* for 10 min at 4°C, and supernatant fluids were stored at −80°C. For Western blot analysis, cells were collected by scraping and low-speed centrifugation. Then, cell pellets were lysed at 4°C in a buffer containing 20 mM Tris–HCl, pH 7.4,

150 mM NaCl, 5 mm EDTA, 5% (v/v) glycerol, 10 mM (v/v) NP-40 and proteases inhibitors cocktail tablets (Roche). The supernatant fraction, obtained by centrifugation at 15,000*g* for 15 min, was stored at −80°C. The protein concentration was determined by the Bio-Rad protein assay according to the supplier's manual (Bio-Rad, Milan, Italy).

Electrophoretic Mobility-Shift Assay (EMSA)

Plasmid pSPT-fer containing the sequence corresponding to the IRE of the H-chain of human ferritin, linearized at the *Bam*HI site, was transcribed in vitro as previously described [Festa et al., 2000a]. For RNA–protein band-shift analysis, cytosolic extracts (5 μg) were incubated for 30 min at room temperature with 0.2 ng of in vitro-transcribed ^{32}P-labelled IRE RNA. The reaction was performed in buffer containing 10 mM HEPES, pH 7.5, 3 mM $MgCl_2$, 40 mM KCl, 5% (v/v) glycerol, 1 mM DTT and 0.07% (v/v) NP-40, in a final volume of 20 μl. To recover total IRP-1 binding activity, cytosolic extracts were pre-incubated for 10 min with 2-mercaptoethanol (2-ME) at a 2% (v/v) final concentration, before the addition of ^{32}P-labelled IRE RNA. Unbound RNA was digested for 10 min with 1 U RNase T_1 (Roche), and non-specific RNA–protein interactions were displaced by the addition of 5 mg/ml heparin for 10 min. RNA–protein complexes were separated on 6% non-denaturing polyacrylamide gel for 2 h at 200 V. After electrophoresis, the gel was dried and autoradiographed at −80°C. The IRPs–IRE complexes were quantified with a GS-700 imaging densitometer and/or with a GS-505 molecular imager system (Bio-Rad). The results are expressed as the percentage of IRP-1 binding activity versus 2-mercaptoethanol-treated samples.

Western Blot Analysis

Samples containing 100 μg of proteins were denatured, separated on a 12% (for ferritin) or 8% (for IRP-1 and TfR-1) SDS–polyacrylamide gel and electro-transferred onto a nitrocellulose membrane (Amersham Biosciences, Little Chalfont, Buckinghamshire, UK) using a Bio-Rad Transblot (Bio-Rad, Milan, Italy). Proteins were visualized on the filters by reversible staining with Ponceau-S solution and destained in PBS. Membranes were blocked at room temperature in milk buffer [1× PBS, 10% (w/v) non-fat dry milk, 0.1% (v/v) Triton X-100] and then incubated at 4°C overnight with 1:1,000 rabbit polyclonal antibody to human ferritin (DakoCytomation, Glostrup, Denmark), or with 1:1,000 mouse antibody to human transferrin receptor-1 (Zymed Laboratories Inc., CA, USA), or with 1:250 goat antibody to human IRP-1 (Santa Cruz Biotechnology, Inc., Santa Cruz, CA, USA). Subsequently, the membranes were incubated for 90 min at room temperature with peroxidase-conjugated goat anti-mouse IgG + IgM, or peroxidase-conjugated rabbit anti-goat IgG, or peroxidase-conjugated goat anti-rabbit IgG (all the secondary antibodies were purchased from Jackson ImmunoResearch Laboratories, Baltimore Pike, West Grove, PA). The resulting complexes were visualized using chemoluminescence Western blotting detection reagents (ECL, Amersham Biosciences). The optical density of the bands was determined by a GS-700 imaging densitometer (Bio-Rad). Normalisation of results was ensured by incubating the nitrocellulose membrane in parallel with the β-actin antibody.

Cellular Labile Iron Pool (LIP) Evaluation

The cellular labile iron content was estimated by a fluorimetric assay using the metal-sensitive probe calcein (CA) and the strong membrane-permeant iron chelator BIP (2,2′-bipyridil, Sigma–Aldrich) [Esposito et al., 2002]. After established times of BHV-1 infection (using a MOI of 1), MDBK cells plated at a density of 1.5×10^3 cells/well were loaded with 0.5 μM CA-AM (calcein-acetomethoxy, Molecular Probes, Eugene, OR) for 30 min at 37°C in calcium- and bicarbonate-free modified Krebs-Henseleit buffer (KHB) consisting of 20 mM HEPES, pH 7.4, 119 mM NaCl, 4.9 mM KCl, 0.96 mM KH_2PO_4 and 5 mM glucose. CA-AM rapidly penetrates across the plasma membrane and is intracellularly hydrolysed to release free CA. After loading, the cultures were washed of excess CA-AM three times with KHB. Cellular CA fluorescence was recorded in a Perkin Elmer microplate reader (Perkin Elmer LS 55 Luminescence Spectrometer, Beaconsfield, UK) using a filter combination with an excitation wavelength of 485 nm and an emission wavelength of 530 nm (slits 5 nm). Cell cultures without CA-AM were used as blank to correct non-specific autofluorescence. Trypan blue was added in all experiments to eliminate extra-cellular CA fluorescence.

The calcein-loaded cells have a fluorescence component (ΔF) that is quenched by intra-

cellular iron and can be revealed by addition of 100 μM BIP. The rise in fluorescence is equivalent to the change in calcein concentration or to the amount of cell iron originally bound to CA [Breuer et al., 1995b]. Thus, the changes in CA fluorescence intensity was directly proportional to the iron labile pool. To characterize the responsiveness of CA fluorescence toward different concentrations of intracellular iron, cells were preloaded with ferrous ammonium sulphate, ferric ammonium citrate or with the cell-permeable ferrous iron chelator BIP.

Statistical Analysis

For the MTT assay and LIP determination, results are expressed as mean ± standard error of the mean (SEM) of n observations, where n represents the number of experiments performed on different days. Triplicate wells were used for the different treatment conditions. The results were analysed by one-way ANOVA followed by a Bonferroni post hoc test for multiple comparisons. A *P*-value less than 0.05 was considered significant.

The densitometric data from EMSA and Western blot are reported as arbitrary units ± standard error of the mean (SEM) of n observations, where n represents the number of experiments performed on different days. Statistical significance among the results was determined by the ANOVA followed by the Newman–Keuls test. A *P*-value less than 0.05 was considered statistically significant.

RESULTS

Effect of BHV-1 Infection on MDBK Cells Viability

We first analysed the effect of BHV-1 infection on MDBK cells survival and viability. Cell viability was investigated by measuring the mitochondrial redox capacity with the MTT assay. To this aim, monolayers of MDBK cells were infected with BHV-1 Cooper at a multiplicity of infection (MOI) of 0.01, 0.1, 1 and 10, then MTT assays were performed at different times post-infection (p.i.). The obtained results, displayed in Figure 1, showed a marked mitochondrial suffering at 48 h p.i. at the highest employed MOI (10), with a decrease of mitochondrial dehydrogenases activity of around 90%. At the same time p.i., the mitochondrial impairment was significant for all the tested MOI with respect to control cells. A significant decrease of mitochondrial dehydrogenases activity was observed as well at 24 h p.i. using a MOI of 0.1, 1 and 10. Moreover, a significant reduction of mitochondrial dehydrogenases activity was already detectable at 12 h after BHV-1 infection but only using the highest MOI (10). Shorter times post-infection (3 and 6 h) did not cause any appreciable mitochondrial suffering at all the tested MOI. Therefore, because of the overt cytopathic effect of Cooper strain in MDBK cells at a MOI of 10 and considering that a MOI of 1 was effective to give productive infection yet not extremely cytopathic, we used a MOI of 1 in all the experiments described herein.

Throughout the in vitro experiments, confluent monolayers of MDBK cells infected with BHV-1 were examined under phase-contrast light microscopy. The data on cell viability by MTT assay were supported by microscopic analysis of living cells infected with BHV-1. In fact, as reported in the micrographs of Figure 2, in vitro modification of the morphology of MDBK monolayers clearly appeared. Prolonged virus infections at a MOI of 1 induced a cytopathic effect already detectable at 24 h p.i., which became very marked at 72 h p.i. leading to whole destruction of cellular monolayer.

Iron Regulatory Proteins Activity and Expression During BHV-1 Infection

In order to examine the possible misregulation of cellular iron homeostasis and the correlation with cell viability during viral infection, we evaluated the effect of BHV-1 infection on IRPs activity. To this aim, we exposed MDBK cells to BHV-1 infection at a MOI of 1, and then we analysed at different times p.i. (0.5, 1, 2, 3, 5, 7, 16, 24, 48 h) the RNA-binding activity of IRPs on cell lysates by means of EMSA. The results are shown in Figure 3. Virus infection caused a time-dependent decrease of IRP-1 RNA-binding activity. This effect already appeared after 30 min of infection, became significant at 3 h p.i. (26% decrease vs. control) and persisted up to 48 h, reaching the minimum of IRP-1 activity after 16 h of BHV-1 infection (45% decrease vs. control). To determine the total amount of IRP-1 RNA-binding activity, 2-mercaptoethanol was added to the binding reaction before the addition of ^{32}P-labelled IRE to reveal "latent" IRP-1 RNA-binding activity, thus giving the total amount of

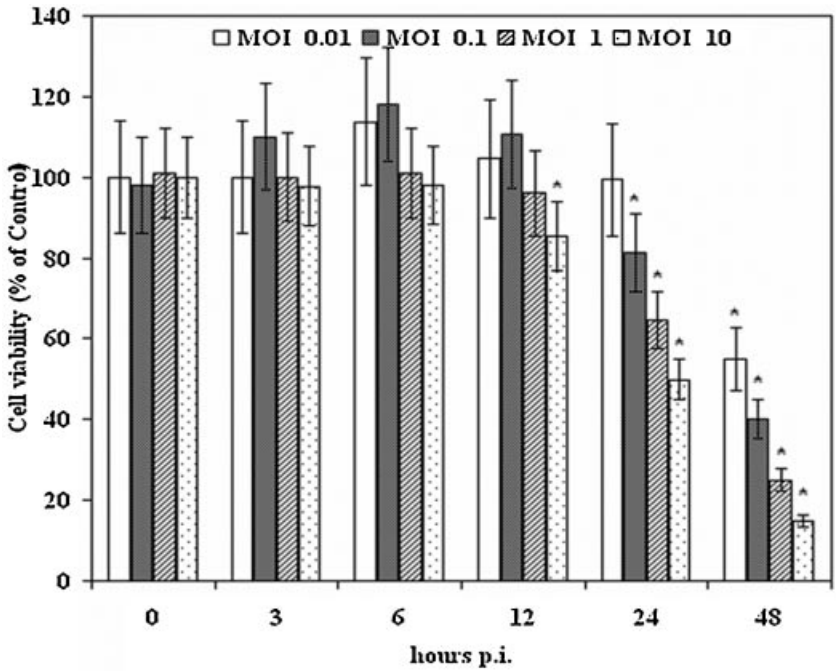

Fig. 1. MDBK cells were incubated for the indicated times with various MOI of BHV-1. After incubations, cell viability was evaluated with MTT assay. Results are expressed in bar graph as the percentage of cell viability to control cultures ± SEM (n = 6) of four independent experiments. $^{*}P \leq 0.05$ versus control cells.

IRP-1 activity (100% of IRE-binding). Concomitant with the early decrease of IRP-1 binding capacity, we found a significant infection-dependent increase in IRP-2 RNA-binding activity, mainly detectable between 30 min and 2 h p.i. Interestingly, the extent of IRP-2 activity appeared extremely variable during prolonged virus infection, with a visible up-regulation yet again at 16 h. This modulation of IRP-2 activity could be due to the accumulation of IRP-2 protein as a consequence of a virus dependent decrease in IRP-2 ubiquitination even though the possibility cannot be excluded that IRP-2 binding activity may itself be subjected to as yet unidentified regulatory mechanism induced by BHV-1 infection. It should be noted that 2-ME treatment decreases IRP-2 activity in proteic cell extracts. This phenomenon could be explained by the sensitivity of IRP-2 to redox status. In fact, routine in vitro

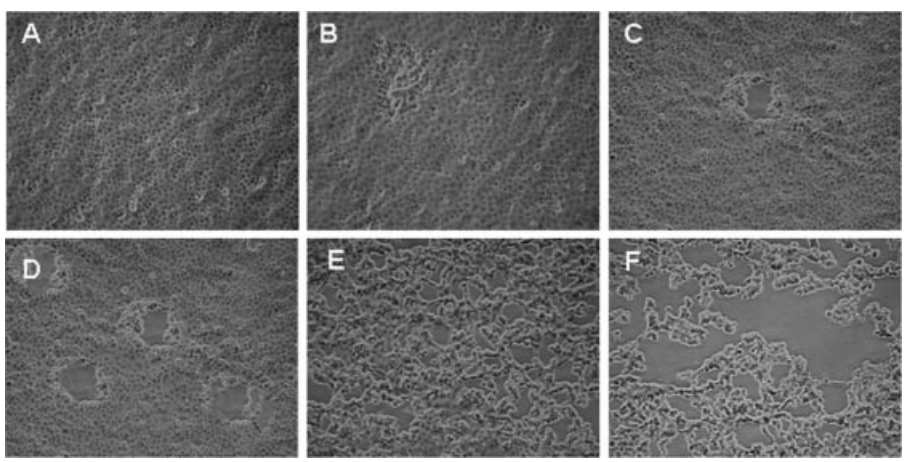

Fig. 2. Microphotographs by phase-contrast light microscopy of MDBK cells at 0, 6, 12, 24, 48 and 72 h post-BHV-1 infection with a MOI of 1 (panels **A**, **B**, **C**, **D**, **E** and **F**, respectively). The cytopathic effect was detectable on the cell monolayer morphology starting from 24 h post-infection.

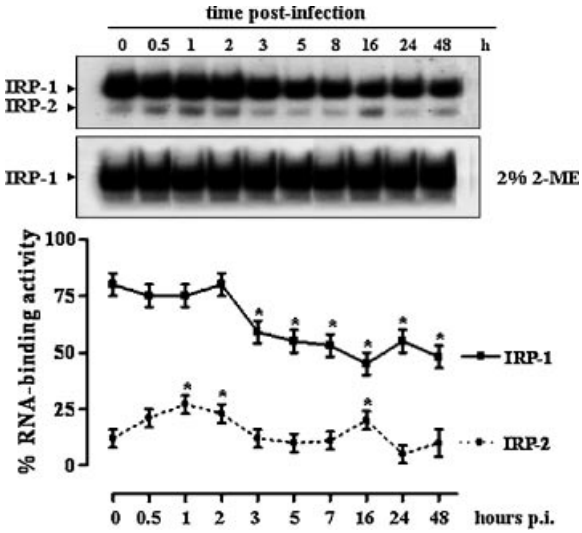

Fig. 3. IRP-1 and IRP-2 RNA-binding activity in MDBK cells during BHV-1 infection. RNA band-shift assay was performed with 5 μg of cytoplasmic proteins and an excess of ^{32}P-labelled IRE probe in absence or presence of 2% 2-ME. RNA–protein complexes were separated on non-denaturing 6% polyacrylamide GEL and revealed by autoradiography. IRP1-RNA and IRP2-RNA complexes were then quantified by densitometric and/or PhosphorImager analysis. The results of experiments performed without 2-ME were plotted in a graph as percent of the control treated with 2-ME and are the average ± SEM values of four independent experiments (solid line IRP-1; dotted line IRP-2). Control treated with 2-ME represents the 100% of IRP-1 RNA-binding activity. The autoradiograms shown are representative of four experiments. *$P < 0.05$ compared with controls.

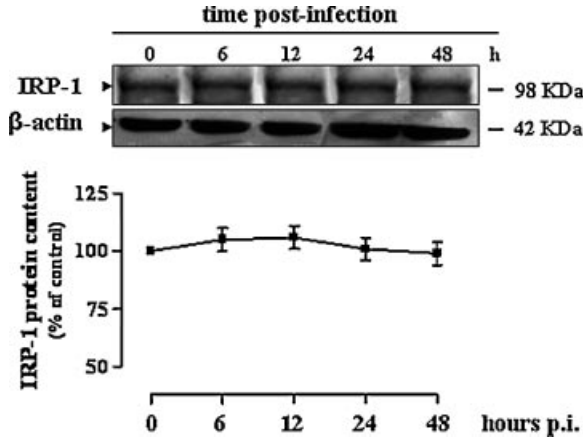

Fig. 4. Western blot analysis showing the effect of BHV-1 infection on IRP-1 protein content in MDBK cells for the indicated times. Equal amounts of proteins (100 μg) were separated on a 8% SDS–polyacrylamide gel and subjected to Western blot analysis using 1:250 dilution of IRP-1 antiserum. β-Actin was used as internal control to standardize the amounts of proteins in each lane. Shown are the means ± SEM of four independent experiments plotted in a graph as percent of control cultures.

treatment of cell extracts with 2% 2-ME, useful to maximally activate IRP-1 RNA-binding activity, results in underestimation of IRP-2 activity [Bouton et al., 1997; Irace et al., 2005].

However, taken all together these results showed an overall decrease of IRPs RNA-binding activity through BHV-1 infection. To evaluate whether the modulation of IRP-1 RNA-binding activity was caused by an infection-induced variation of IRP-1 protein content, we successively analysed the IRP-1 levels in MDBK cells exposed to BHV-1 for the indicated times. As shown in Figure 4, immunoblot analysis did not show any appreciable variations in the amounts of IRP-1 protein in all the examined samples, suggesting that BHV-1 infection in mammalian cells caused a regulation of RNA-binding activity of IRP-1 without affecting the protein expression.

Ferritin and TfR-1 Expression are Regulated Post-Transcriptionally by BHV-1 Infection

To evaluate ferritin and TfR-1 expression during the BHV-1 infection of the MDBK cells, we determined the levels of these proteins by Western blot analysis on lysates obtained from infected cells (MOI of 1) for different times. As shown in Figure 5, BHV-1 infection significantly increased ferritin levels progressively, a maximum being reached at 48 h p.i. Bovine kidney cell lysates showed an electrophoretic pattern in which the H- and L-ferritin subunits overlapped, and ferritin content increased by about 1.3-, 1.5- and 1.6-fold after 12, 24 and 48 h p.i., respectively.

Concomitantly, immunoblot analysis of TfR-1 showed a remarkable time-dependent decrease of the protein levels following virus infection. As shown in Figure 5 at 48 h p.i. there is evidence for a reduction of TfR-1 content of about 60% respect to control cells. These results are consistent with the hypothesis that the overall infection-induced decrease of IRE-binding activity of IRPs leads to an increased ferritin mRNA translation and to a simultaneous decreased TfR-1 mRNA translation.

Evaluation of Cellular Labile Iron Pool During BHV-1 Infection

The decrease of TfR-1 protein and the ferritin induction following the BHV-1 infection, could lead to an alteration of the LIP extent. Therefore, we next evaluated the magnitude of the LIP with the CA assay, which is based on the principle that the CA loaded into cell binds a large fraction of the LIP. The CA-bound iron is

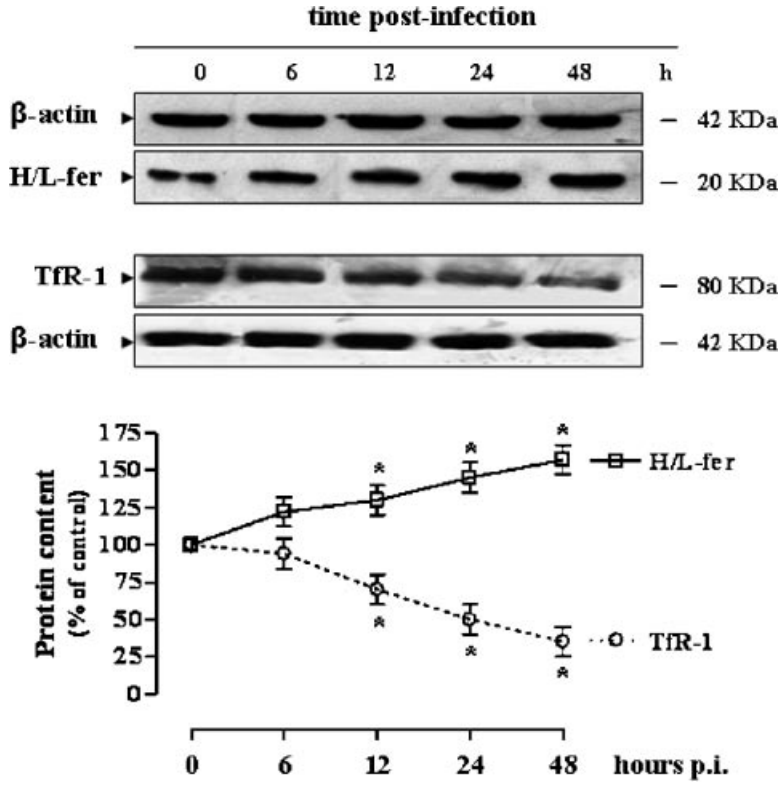

Fig. 5. Western blot analysis showing the ferritin (H/L-fer) and the transferrin receptor-1 (TfR-1) levels in MDBK cells for the post-infection indicated times. For ferritin content analysis, equal amounts of cytosolic lysates containing 100 μg of proteins were fractionated by 12% SDS–PAGE and subjected to Western blot analysis using 1:1,000 dilution of ferritin antiserum. For TfR-1 content analysis, equal amounts of cytosolic lysates containing 100 μg of proteins were fractionated by 8% SDS–PAGE and subjected to Western blot analysis using 1:1,000 dilution of TfR-1 antiserum. H/L-fer and TfR-1 were detected by chemoluminescence, the corresponding bands were then quantified by densitometric analysis and plotted as percentage of control (solid line ferritin; dotted line TfR-1). The anti-β-actin antibody was used to standardize the amounts of proteins in each lane. Shown are the average ± SEM values of four independent experiments and the Western blots shown are representative of four experiments. *$P < 0.05$ versus control cells.

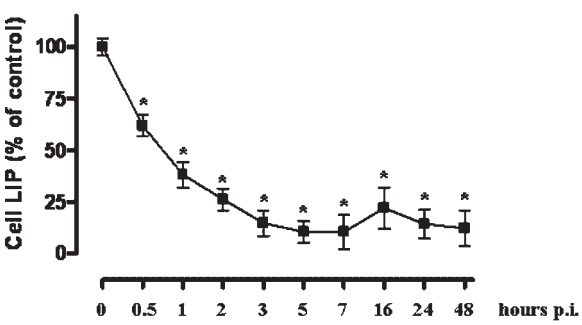

Fig. 6. LIP extent following BHV-1 infection (MOI of 1) in MDBK cells estimated for the indicated times with the CA fluorescent method. Cell cultures were loaded with CA using acetomethoxyl-calcein, and fluorescence was measured before and after the addition of 100 μM permeant iron chelator BIP. Shown are the average ± SEM (n = 6) values of three independent experiments plotted in a graph as percent of control cultures. *$P < 0.05$ versus control cells.

revealed by the addition of excess permeant chelator BIP that restores CA's fluorescence. The magnitude of the chelator-mediated rise in fluorescence is proportional to the amount of CA-bound iron and therefore reflects the LIP extent. As clearly shown in Figure 6, the labile iron pool was strongly diminished in MDBK cells during BHV-1 infection. In particular, LIP decreased with a progressive extent throughout the early phase of infection with a diminution of about 60% at 1 h p.i., reaching the lowest level after 5 h p.i.

DISCUSSION

The premise underlying this study is that DNA viruses are directly dependent on iron for their proliferation since this metal plays a crucial role in the catalytic center of ribonucleotide reductase [Cooper et al., 1996; Lamarche et al., 1996; Chabes et al., 2000]. DNA viruses

absolutely require the pools of dNTPs provided by RR for their replicative cycle. In fact, the inactivation of the RR enzyme by hydroxyurea that quenches a tyrosyl radical in the catalytic center, blocks the virus infection [Slabaugh and Mathews, 1986]. Therefore, to give productive infection the RR apoprotein must scavenge iron from the endogenous 'labile iron pool'. Despite the fact that other pathogens such as bacteria and fungi have adapted in several ways to the iron-limited environment [Neilands, 1995; Howard, 1999], viruses have not evolved mechanisms for actively scavenging host iron. In mammalian cells the majority of iron is sequestered into ferritin, and free iron is present in very low amounts (~20% of the total iron in mammalian cells in culture) [Breuer et al., 1995a]. Only a minor fraction of total cell iron is bound as a prosthetic group in iron-containing proteins. Among these, would be ribonucleotide reductase, whether the endogenous eukaryotic enzyme or a pathogen-encoded one.

Changes in iron homeostasis have been implicated in the pathogenesis of several viruses, including hepatitis C, herpes simplex virus, human immunodeficiency virus, rhabdovirus, and vaccinia virus [Laham and Ehrlich, 2004]. Thus, the biosynthesis and the levels of the proteins involved in iron homeostasis, and hence the magnitude of the LIP, may be critical in the development of host cell damage and for productive viral infection.

In the present study we describe that BHV-1 infection in mammalian cells affects regulation of RNA-binding of both IRP-1 and IRP-2. This phenomenon seems not be associated with any appreciable variations in cellular IRP-1 levels thus suggesting that infection status modulates RNA-binding activity of IRP-1 without affecting the protein expression. Concerning IRP-2, it is expected that its content would correlate to intracellular iron [Guo et al., 1995; Wallander et al., 2006]. IRPs primarily respond to changes in iron pool and control the expression of mRNAs containing IRP binding sites (e.g. ferritin and TfR-1), thus setting in play mechanisms to control iron homeostasis.

We have determined that viral infection induced an overall down regulation of IRPs RNA-binding activity leading to an increased ferritin mRNA translation and to a simultaneous decreased TfR-1 mRNA translation. In fact, we found a significant progressive enhancement of ferritin content, which increased of about 1.6-fold respect to control cells after 48 h p.i. As consequence of the decreased IRPs binding to the TfR-1 mRNA, the evaluation of TfR-1 expression during BHV-1 infection showed a marked decrease of this membrane receptor. Since the cellular up-take of iron occurs through receptor mediated endocytosis of diferric-transferrin by the TfR-1, the down-regulation of TfR-1 expression at the cell membrane surface is inevitably associated with a lowered cellular iron up-take [Dunn et al., 2007]. This condition, coupled to ferritin induction, could lead to a physiologically important alteration of the LIP extent. This hypothesis is strongly supported by the finding that the level of LIP, measured by calcein assay, rapidly decrease following BHV-1 infection.

Most likely in this way, by reducing the metal up-take and by enhancing the sequestration of free iron, animal cells limit the iron availability for virus proliferation. Our results are consistent with the hypothesis that cellular organisms increase the levels of iron-binding proteins in order to reduce the iron availability during virus infection [Weinberg, 1996]. In this context, ferritin is the more efficient one and induction of this protein, that acts as an effective Fe^{2+} scavenger by its ability to sequester up to 4,500 iron ions per molecule [Theil, 2004], might interfere with the virus replication by sequestering iron from the endogenous 'LIP' and by reducing iron availability to assemble functional viral RR. A similar effect is observed when membrane-permeant strong iron chelators, such as bipyridyl (BIP) and salicylaldehyde isonicotinoyl hydrazone (SIH), are added to in vitro experiments in a standard plaque assay [Romeo et al., 2001]. An increase of ferritin expression has been also reported by Mulvey et al. [1996] in the mengo virus infections, and more recently the increase of ferritin expression has been correlated with the integrity of the casein kinase II phosphorylation site of the mengo virus leader protein [Zoll et al., 2002].

A large body of evidence has suggested that ferritin can be considered not only as a member of a proteins group involved in the iron metabolism, but also as a member of a protein family that modulates the cellular defence against stress and inflammation. In fact, several regulatory factors, including infections by pathogens, in addition to those that regulate iron homeostasis, may have an important impact on cellular ferritin expression and function [Torti

and Torti, 2002]. Indeed, ferritin gene expression is complex and is controlled at transcriptional and post-transcriptional levels [Harrison and Arosio, 1996]. Moreover, specific regulatory mechanisms also appear to be dependent on cell species and type. Therefore, the ferritin induction, the decrease of TfR-1 expression and the LIP reduction are phenomena beginning early during infection, probably coupled with the activation of the early ribonucleotide reductase gene product that needs iron. Although this cell response could represent a defensive mechanism to BHV-1 infection, it is not effective to counteract viral replication and thus the cytotoxicity becomes evident much later during infection.

On the other hand, perturbations of iron homeostasis induced by virus infection could play a role in immunosuppressive mechanisms, and therefore allowing virus proliferation. Hence, the host iron status and the progression of viral infection seem to be strictly connected. In this scenario, it is noteworthy to consider that ferritin induction during infection could play a pivotal role in immunosuppressive mechanisms, acting as a down-regulator of cellular immunity [Moroz et al., 1989, 2002]. Should be this the case, the enhanced ferritin content found in the MDBK cells upon BHV-1 infection would correlate with the suppression of the antiviral host cell response.

In conclusion, associations between host iron status and viral infection appear to be bidirectional: iron status may alter the severity of disease as well as infection can alter the iron homeostasis [Crowe et al., 2004]. All together, these suggestions confirm the view that the iron metabolism represents an important area for interaction between DNA viruses, such as BHV-1, and mammalian cells. Definition of the relationship among pathogen and host may make available new antimicrobial agents. A hopeful approach involves the understanding of the molecular basis of host iron homeostasis and the mechanisms by which microbial pathogens circumvent these processes.

REFERENCES

Aisen P, Wessling-Resnick M, Leibold EA. 1999. Iron metabolism. Curr Opin Chem Biol 3:200–206.

Aziz N, Munro HN. 1987. Iron regulates ferritin mRNA translation through a segment of its 5′ untranslated region. Proc Natl Acad Sci USA 84:8478–8482.

Bouton C, Hirling H, Drapier JC. 1997. Redox modulation of iron regulatory proteins by peroxynitrite. J Biol Chem 272:19969–19975.

Breuer W, Epsztejn S, Cabantchik ZI. 1995a. Iron acquired from transferrin by K562 cells is delivered into a cytoplasmic pool of chelatable iron (II). J Biol Chem 270:24209–24215.

Breuer W, Epsztejn S, Millgram P, Cabantchik ZI. 1995b. Transport of iron and other transition metals into cells as revealed by a fluorescent probe. Am J Physiol 268:1354–1361.

Brown NM, Anderson SA, Steffen DW, Carpenter TB, Kennedy MC, Walden WE, Eisenstein RS. 1998. Novel role of phosphorylation in Fe-S cluster stability revealed by phosphomimetic mutation at Ser-138 of iron regulatory protein 1. Proc Natl Acad Sci USA 95:15235–15240.

Chabes A, Domkin V, Larsson G, Liu A, Graslund A, Wijmenga S, Thelander L. 2000. Yeast ribonucleotide reductase has a heterodimeric iron-radical-containing subunit. Proc Natl Acad Sci USA 97:2474–2479.

Cinatl J, Jr., Cinatl J, Rabenau H, Gumbel HO, Kornhuber B, Doerr HW. 1994. In vitro inhibition of human cytomegalovirus replication by desferrioxamine. Antiviral Res 25:73–77.

Clark TD, Semba RD. 2001. Iron supplementation during human immunodeficiency virus infection: A double-edged sword? Med Hypotheses 57:476–479.

Cooper CE, Lynagh GR, Hoyes KP, Hider RC, Cammack R, Porter JB. 1996. The relationship of intracellular iron chelation to the inhibition and regeneration of human ribonucleotide reductase. J Biol Chem 271:20291–20299.

Crowe WE, Maglova LM, Ponka P, Russell JM. 2004. Human cytomegalovirus-induced host cell enlargement is iron dependent. Am J Physiol Cell Physiol 287:1023–1030.

Darnell G, Richardson DR. 1999. The potential of iron chelators of the pyridoxal isonicotinoyl hydrazone class as effective antiproliferative agents III: The effect of the ligands on molecular targets involved in proliferation. Blood 94:781–792.

Drapier JC, Hirling H, Wietzerbin J, Kaldy P, Kühn LC. 1993. Biosynthesis of nitric oxide activates iron regulatory factor in macrophages. EMBO J 12:3643–3649.

Dunn LL, Rahmanto YS, Richardson DR. 2007. Iron uptake and metabolism in the new millennium. Trends Cell Biol 17:93–100.

Eisenstein RS. 2000. Iron regulatory proteins and the molecular control of mammalian iron metabolism. Annu Rev Nutr 20:627–662.

Esposito BP, Epsztejn S, Breuer W, Cabantchik ZI. 2002. A review of fluorescence methods for assessing labile iron in cells and biological fluids. Anal Biochem 304:1–18.

Festa M, Ricciardelli G, Mele G, Pietropaolo C, Ruffo A, Colonna A. 2000a. Overexpression of H ferritin and up-regulation of iron regulatory protein genes during differentiation of 3T3-L1 pre-adipocytes. J Biol Chem 275:36708–36712.

Festa M, Colonna A, Pietropaolo C, Ruffo A. 2000b. Oxalomalate, a competitive inhibitor of aconitase, modulates the RNA-binding activity of iron-regulatory proteins. Biochem J 348:315–320.

Fishman JB, Rubin JB, Handrahan JV, Connor JR, Fine RE. 1987. Receptor mediated transcytosis of transferrin across the blood-brain barrier. J Neurosci Res 18:299–304.

Guo B, Yu Y, Leibold EA. 1994. Iron regulates cytoplasmic levels of a novel iron-responsive element-binding protein without aconitase activity. J Biol Chem 269:24252–24260.

Guo B, Phillips JD, Yu Y, Leibold EA. 1995. Iron regulates intracellular degradation of iron regulatory protein 2 by the proteasome. J Biol Chem 270:21645–21651.

Harrison PM, Arosio P. 1996. The ferritins: Molecular properties, iron storage function and cellular regulation. Biochim Biophys Acta 1275:161–203.

Henderson BR, Kühn LC. 1995. Differential modulation of the RNA-binding protein IRP-1 and IRP-2 in response to iron. IRP-2 inactivation require translation of another protein. J Biol Chem 270:20509–20515.

Hentze MW, Rouault TA, Caughman SW, Dancis A, Harford JB, Klausner RD. 1987. A cis-acting element is necessary and sufficient for translational regulation of human ferritin expression in response to iron. Proc Natl Acad Sci USA 84:6730–6734.

Howard DH. 1999. Acquisition, transport, and storage of iron by pathogenic fungi. Clin Microbiol Rev 12:394–404.

Howell ML, Roseman NA, Slabaugh MB, Mathews CK. 1993. Vaccinia virus ribonucleotide reductase. Correlation between deoxyribonucleotide supply and demand. J Biol Chem 268:7155–7162.

Irace C, Scorziello A, Maffettone C, Pignataro G, Matrone C, Adornetto A, Santamaria R, Annunziato L, Colonna A. 2005. Divergent modulation of iron regulatory proteins and ferritin biosynthesis by hypoxia/reoxygenation in neurons and glial cells. J Neurochem 95:1321–1331.

Jones C. 2003. Herpes simplex virus type 1 and bovine herpesvirus 1 latency. Clin Microbiol Rev 16:79–95.

Kakizaki S, Takagi H, Horiguchi N, Toyoda M, Takayama H, Nagamine T, Mori M. 2000. Iron enhances hepatitis C virus replication in cultured human hepatocytes. Liver 20:25–128.

Kennedy MC, Mende-Mueller L, Blodin GA, Beinert H. 1992. Purification and characterization of cytosolic aconitase from beef liver and its relationship to the iron-responsive element binding protein. Proc Natl Acad Sci USA 89:11730–11734.

Laham N, Ehrlich R. 2004. Manipulation of iron to determine survival: Competition between host and pathogen. Immunol Res 30:15–28.

Lamarche N, Matton G, Massie B, Fontecave M, Atta M, Dumas F, Gaudreau P, Langelier Y. 1996. Production of the R2 subunit of ribonucleotide reductase from herpes simplex virus with prokaryotic and eukaryotic expression systems: Higher activity of R2 produced by eukaryotic cells related to higher iron-binding capacity. Biochem J 320:129–135.

McGeoch DJ, Davison AJ. 1999. The molecular evolutionary history of the herpesviruses. In: Domingo E, Webster R, Holland J, editors. Origin and evolution of viruses. London: Academic Press. pp 441.

Meyron-Holtz EG, Ghosh MC, Rouault TA. 2004. Mammalian tissue oxygen levels modulate iron-regulatory protein activities in vivo. Science 306:2087–2090.

Moroz C, Misrock SL, Siegal FP. 1989. Isoferritins in HIV infection: Relation to clinical stage, CD8 lymphocyte binding and the pathogenesis of AIDS. AIDS 3:11–16.

Moroz C, Traub L, Maymon R, Zahalka MA. 2002. PLIF, a novel human ferritin subunit from placenta with immunosuppressive activity. J Biol Chem 277:12901–12905.

Müllner EW, Neupert B, Kühn LC. 1989. A specific mRNA binding factor regulates the iron-dependent stability of cytoplasmic transferrin receptor mRNA. Cell 58:373–382.

Mulvey MR, Kuhn LC, Scraba DG. 1996. Induction of ferritin synthesis in cells infected with Mengo virus. J Biol Chem 271:9851–9857.

Neilands JB. 1995. Siderophores: Structure and function of microbial iron transport compounds. J Biol Chem 270: 26723–26726.

Nelson SK, McCord JM. 1998. Iron, oxygen radicals, and disease. Adv Mol Cell Biol 25:157–183.

Pantopoulos K. 2004. Iron metabolism and the IRE/IRP regulatory system: An update. Ann NY Acad Sci 1012:1–13.

Pantopoulos K, Mueller S, Atzberger A, Ansorge W, Stremmel W, Hentze MW. 1997. Differences in the regulation of iron regulatory protein-1 (IRP1) by extra- and intra-cellular oxidative stress. J Biol Chem 272: 9802–9808.

Richardson DR. 1997. Potential of iron chelators as effective antiproliferative agents. Can J Physiol Pharmacol 75:1164–1180.

Roizman B, Pellet P. 2001. The family herpesviridae: A brief introduction. In: Knipe DM, Howley PM, editors. Fields' virology 4th edition. Philadelphia: Lippincott Williams & Wilkins. pp 2381–2397.

Romeo AM, Christen L, Niles EG, Kosman DJ. 2001. Intracellular chelation of iron by bipyridyl inhibits DNA virus replication. J Biol Chem 276:24301–24308.

Santamaria R, Irace C, Festa M, Maffettone C, Colonna A. 2004. Induction of ferritin expression by oxalomalate. Biochim Biophys Acta 1691:151–159.

Santamaria R, Bevilacqua MA, Maffettone C, Irace C, Iovine B, Colonna A. 2006. Induction of H-ferritin synthesis by oxalomalate is regulated at both the transcriptional and post-transcriptional levels. Biochim Biophys Acta 1763:815–822.

Slabaugh MB, Mathews CK. 1986. Hydroxyurea-resistant vaccinia virus: Overproduction of ribonucleotide reductase. J Virol 60:506–514.

Stubbe J. 1990. Ribonucleotide reductases: Amazing and confusing. J Biol Chem 265:5329–5332.

Theil EC. 2004. Iron, ferritin, and nutrition. Annu Rev Nutr 24:327–343.

Torti FM, Torti SV. 2002. Regulation of ferritin genes and protein. Blood 99:3505–3516.

Van Asbeck BS, Georgiou NA, van der Bruggen T, Oudshoorn M, Nottet HS, Marx JJ. 2001. Anti-HIV effect of iron chelators: Different mechanisms involved. J Clin Virol 20:141–147.

Wallander ML, Leibold EA, Eisenstein RS. 2006. Molecular control of vertebrate iron homeostasis by iron regulatory proteins. Biochim Biophys Acta 1763:668–689.

Weinberg ED. 1996. Iron withholding: A defense against viral infections. Biometals 9:393–399.

Weiss G, Umlauft F, Urbanek M, Herold M, Lovevsky M, Offner F, Gordeuk VR. 1999. Associations between cellular immune effector function, iron metabolism, and disease activity in patients with chronic hepatitis C virus infection. J Infect Dis 180:1452–1458.

Zoll J, Melchers WJG, Galama JMD, van Kuppeveld FJM. 2002. The mengovirus leader protein suppresses alpha/beta interferon production by inhibition of the iron/ferritin-mediated activation of NF-κB. J Virol 76:9664–9672.